A convergent algorithm for mean curvature flow driven by diffusion on the surface

Balázs Kovács
Mathematisches Institut, Universität Tübingen,
Auf der Morgenstelle 10, 72076 Tübingen, Germany
kovacs@na.uni-tuebingen.de

Buyang Li

Department of Applied Mathematics,
The Hong Kong Polytechnic University, Hong Kong
buyang.li@polyu.edu.hk

Christian Lubich

Mathematisches Institut, Universität Tübingen,
Auf der Morgenstelle 10, 72076 Tübingen, Germany
lubich@na.uni-tuebingen.de

July 4, 2022

Abstract

The evolution of a closed two-dimensional surface driven by both mean curvature flow and a reaction—diffusion process on the surface is formulated into a system, which couples the velocity law not only to the surface partial differential equation but also to the evolution equations for the geometric quantities, namely the normal vector and the mean curvature on the surface. Two algorithms are considered for the obtained system. Both methods combine surface finite elements as a space discretisation and linearly implicit backward difference formulae for time integration. Based on our recent results for mean curvature flow, one of the algorithms directly admits a convergence proof for its full discretisation in the case of finite elements of polynomial degree at least two and backward difference formulae of orders two to five. Numerical examples are provided to support and complement the theoretical convergence results (demonstrating the convergence properties of the method without error estimate), and demonstrate the effectiveness of the methods in simulating a three-dimensional tumour growth model.

2010 Mathematics Subject Classification: Primary 35R01; 65M60; 65M15; 65M12.

Keywords: forced mean curvature flow; reaction–diffusion on surfaces; evolving finite element method; linearly implicit; backward difference formula; convergence; tumour growth.

1 Introduction

We consider numerical approximation to the evolution of a surface $\Gamma[X]$, determined by a flow map X, driven by both mean curvature flow and a reaction–diffusion problem on the surface. That is, the surface velocity is given by the velocity law

$$v = -H\nu + g(w)\nu, \tag{1.1}$$

where H is the mean curvature and ν is the normal vector of the surface $\Gamma[X]$, and where $g: \mathbb{R} \to \mathbb{R}$ is a given function of w the solution of the nonlinear reaction–diffusion equation

$$\partial^{\bullet} w + w \nabla_{\Gamma[X]} \cdot v - \Delta_{\Gamma[X]} w = F(w, \nabla_{\Gamma[X]} w) \quad \text{on} \quad \Gamma[X], \tag{1.2}$$

with a given nonlinear function $F : \mathbb{R} \times \mathbb{R}^3 \to \mathbb{R}$. Problem (1.1)–(1.2) can be viewed as *forced* mean curvature flow.

Numerical approximation to the mean curvature flow — i.e. the case $g(w) \equiv 0$ in (1.1) — was first addressed in 1990 by Dziuk [13], who proposed a finite element method based on an approximation of the mean curvature flow as a heat equation on a surface, in which the moving nodes of the finite element mesh determine the approximate evolving surface. However, proving convergence of Dziuk's method or of other surface finite element based methods, such as the method proposed by Barrett, Garcke & Nürnberg [4] based on different variational formulations, or the method of Elliott & Fritz [18] based on DeTurck's trick of re-parametrizing the surface, has remained an open problem for the mean curvature flow of closed two-dimensional surfaces.

In [23] we proved the first optimal-order convergence estimates for semi- and full discretisations of mean curvature flow of closed surfaces, by considering the coupled system for the velocity law together with evolution equations for the geometric quantities ν and H, the normal vector and mean curvature.

Many practical applications concern mean curvature flow coupled with surface partial differential equations (PDEs), for example: tumour growth [7, 8, 6, 2]; surface dissolution [19, 17] (also see [15, Section 10.4]); diffusion induced grain boundary motion [20, 10, 29]; sharp interface limit of a perturbed Allen–Cahn equation [27]; etc. Numerical approximation to such forced mean curvature flow coupled with surface PDEs have been considered in some of these papers. For *curves*, convergence of numerical methods for such coupled problems was proved for forced curve shortening flow in [28, 3].

Convergence results, up to our knowledge, have not yet been proved for forced mean curvature flow of closed surfaces without regularization. For a *regularized* version of forced mean curvature flow of closed surfaces optimal-order convergence results for semi- and full discretisations were obtained in [24] and [25], respectively.

In this paper, we extend the approach and techniques of our previous paper [23] to the forced mean curvature flow problem (1.1)–(1.2) as a coupled problem, together with evolution equations for the normal vector and mean curvature. These evolution equations, as compared to mean curvature flow, cf. [22], contain additional forcing terms depending on w. We present two fully discrete evolving finite element algorithms for the obtained coupled system. The first algorithm combines the two terms $\partial^{\bullet}w + w\nabla_{\Gamma[X]}\cdot v$ in spatial discretization by an idea of [14] treating conservation laws on an evolving surface. The second algorithm discretises the two

terms separately in spatial discretization by using the velocity law for v and the approach in [23]. Both algorithms use evolving surface finite elements for spatial discretization and linearly implicit backward difference formulae for time integration, and for both algorithms the moving nodes of a finite element mesh determine the approximate evolving surface.

We show that the second algorithm can be written in the same matrix-vector form as the method proposed in [23] for the mean curvature flow. Thus the convergence analysis in [23] applies directly to the present algorithm for forced mean curvature flow as well. This yields uniform in time, optimal-order H^1 norm convergence results for the semi- and full discretisations of forced mean curvature flow, using at least quadratic evolving surface FEM and linearly implicit backward difference formulae of order two to five. For the first algorithm, we show a similar optimal-order convergence estimate of the evolving surface finite element semi-discretisation.

Finally, we present numerical experiments to support and complement the theoretical results. We present convergence tests for both algorithms, and also present an experiment with the numerical simulation for tumour growth model, using the parameters in [2] for the sake of easy comparison.

2 Evolution equations for mean curvature flow driven by diffusion on the surface

2.1 Basic notions and notation

We consider the evolving two-dimensional closed surface $\Gamma[X] \subset \mathbb{R}^3$ as the image

$$\Gamma[X] = \Gamma[X(\cdot,t)] = \{X(p,t) \,:\, p \in \Gamma^0\},$$

of a smooth mapping $X:\Gamma^0\times[0,T]\to\mathbb{R}^3$ such that $X(\cdot,t)$ is an embedding for every t. Here, Γ^0 is a smooth closed initial surface, and X(p,0)=p. In view of the subsequent numerical discretization, it is convenient to think of X(p,t) as the position at time t of a moving particle with label p, and of $\Gamma[X]$ as a collection of such particles.

The velocity $v(x,t) \in \mathbb{R}^3$ at a point $x = X(p,t) \in \Gamma[X(\cdot,t)]$ equals

$$\partial_t X(p,t) = v(X(p,t),t). \tag{2.1}$$

For a known velocity field v, the position X(p, t) at time t of the particle with label p is obtained by solving the ordinary differential equation (2.1) from 0 to t for a fixed p.

For a function u(x,t) $(x \in \Gamma[X], 0 \le t \le T)$ we denote the *material derivative* (with respect to the parametrization X) as

$$\partial^{\bullet} u(x,t) = \frac{\mathrm{d}}{\mathrm{d}t} \, u(X(p,t),t) \quad \text{ for } x = X(p,t).$$

On any regular surface $\Gamma \subset \mathbb{R}^3$, we denote by $\nabla_{\Gamma} u : \Gamma \to \mathbb{R}^3$ the tangential gradient of a function $u : \Gamma \to \mathbb{R}$, and in the case of a vector-valued function $u = (u_1, u_2, u_3)^T : \Gamma \to \mathbb{R}^3$, we let $\nabla_{\Gamma} u = (\nabla_{\Gamma} u_1, \nabla_{\Gamma} u_2, \nabla_{\Gamma} u_3)$. We thus use the convention that the gradient of u has the gradient of the components as column vectors. We denote by $\nabla_{\Gamma} \cdot f$ the surface divergence of

a vector field f on Γ , and by $\Delta_{\Gamma}u = \nabla_{\Gamma} \cdot \nabla_{\Gamma}u$ the *Laplace–Beltrami operator* applied to u; see the review [9] or [16, Appendix A] or any textbook on differential geometry for these notions.

We denote the unit outer normal vector field to Γ by $\nu:\Gamma\to\mathbb{R}^3$. Its surface gradient contains the (extrinsic) curvature data of the surface Γ . At every $x\in\Gamma$, the matrix of the extended Weingarten map,

$$A(x) = \nabla_{\Gamma} \nu(x),$$

is a symmetric 3×3 matrix (see, e.g., [30, Proposition 20]). Apart from the eigenvalue 0 with eigenvector ν , its other two eigenvalues are the principal curvatures κ_1 and κ_2 . They determine the fundamental quantities

$$H := \operatorname{tr}(A) = \kappa_1 + \kappa_2, \qquad |A|^2 = \kappa_1^2 + \kappa_2^2,$$
 (2.2)

where |A| denotes the Frobenius norm of the matrix A. Here, H is called the *mean curvature* (as in most of the literature, we do not put a factor 1/2).

2.2 Evolution equations for normal vector and mean curvature of a surface moving under mean curvature flow driven by diffusion on the surface

Mean curvature flow driven by diffusion on the surface, or for short forced mean curvature flow, sets the velocity (2.1) of the surface $\Gamma[X]$ to

$$v = -H\nu + g(w)\nu = -V\nu, \tag{2.3}$$

where V denotes the normal velocity, and where the term involving w is an external forcing, with a given function $g: \mathbb{R} \to \mathbb{R}$. Here, w is the solution of the non-linear reaction–diffusion equation on the surface $\Gamma[X]$:

$$\partial^{\bullet} w + w \nabla_{\Gamma[X]} \cdot v - \Delta_{\Gamma[X]} w = F(w, \nabla_{\Gamma[X]} w), \quad \text{on} \quad \Gamma[X], \tag{2.4}$$

where $F: \mathbb{R} \times \mathbb{R}^3 \to \mathbb{R}$ is a given function.

The geometric quantities H and ν on the right-hand side of (2.3) satisfy the following evolution equations, which are modifications of the classical evolution equations for pure mean curvature flow (i.e., $\nu = -H\nu$), cf. Huisken [22].

Lemma 2.1. For a regular surface $\Gamma[X]$ moving under forced mean curvature flow, the normal vector and the mean curvature satisfy

$$\partial^{\bullet} \nu = \Delta_{\Gamma[X]} \nu + |A|^2 \nu - \nabla_{\Gamma[X]} (g(w)), \tag{2.5}$$

$$\partial^{\bullet} H = \Delta_{\Gamma[X]} H + |A|^2 H - \Delta_{\Gamma[X]} (g(w)) - |A|^2 g(w). \tag{2.6}$$

Proof. By using the normal velocity V in the proof of [22, Lemma 3.3], or see also [5, Lemma 2.37], the following evolution equation for the normal vector holds:

$$\partial^{\bullet} \nu = \nabla_{\Gamma[X]} V.$$

On any surface Γ , it holds true that (see [16, (A.9)] or [30, Proposition 24])

$$\nabla_{\Gamma[X]}H = \Delta_{\Gamma[X]}\nu + |A|^2\nu,$$

which, in combination with V = H - g(w) from (2.3), then gives the stated evolution equation for ν .

By revising the proof of [22, Theorem 3.4 and Corollary 3.5], or see [5, Lemma 2.39], with the normal velocity V we obtain

$$\partial^{\bullet} H = \Delta_{\Gamma[X]} V + |A|^2 V,$$

which, again combined with V = H - g(w) from (2.3), yields the evolution equation for H. \square

2.3 The system of equations used for discretization

Similarly as in [23], collecting the above equations, we have reformulated forced mean curvature flow as the system of semi-linear parabolic equations (2.5)–(2.6) on the surface coupled to the velocity law (2.3) and the surface PDE (2.4). The numerical discretization is based on a weak formulation of (2.3)–(2.6), together with the velocity equation (2.1):

$$\int_{\Gamma[X]} \nabla_{\Gamma[X]} v \cdot \nabla_{\Gamma[X]} \varphi^{v} + \int_{\Gamma[X]} v \cdot \varphi^{v} = -\int_{\Gamma[X]} \nabla_{\Gamma[X]} ((H - g(w))\nu) \cdot \nabla_{\Gamma[X]} \varphi^{v}
- \int_{\Gamma[X]} (H - g(w))\nu \cdot \varphi^{v}$$
(2.7a)

$$\int_{\Gamma[X]} \partial^{\bullet} \nu \cdot \varphi^{\nu} + \int_{\Gamma[X]} \nabla_{\Gamma[X]} \nu \cdot \nabla_{\Gamma[X]} \varphi^{\nu} = \int_{\Gamma[X]} |\nabla_{\Gamma[X]} \nu|^{2} \nu \cdot \varphi^{\nu} - \int_{\Gamma[X]} \nabla_{\Gamma[X]} (g(w)) \cdot \varphi^{\nu} \quad (2.7b)$$

$$\int_{\Gamma[X]} \partial^{\bullet} H \varphi^{H} + \int_{\Gamma[X]} \nabla_{\Gamma[X]} H \cdot \nabla_{\Gamma[X]} \varphi^{H} = \int_{\Gamma[X]} |\nabla_{\Gamma[X]} \nu|^{2} (H - g(w)) \varphi^{H}$$

$$+ \int_{\Gamma[X]} \nabla_{\Gamma[X]} (g(w)) \cdot \nabla_{\Gamma[X]} \varphi^{H}, \quad (2.7c)$$

$$\frac{\mathrm{d}}{\mathrm{d}t} \int_{\Gamma[X]} w \varphi^w + \int_{\Gamma[X]} \nabla_{\Gamma[X]} w \cdot \nabla_{\Gamma[X]} \varphi^w = \int_{\Gamma[X]} F(w, \nabla_{\Gamma[X]} w) \varphi^w, \tag{2.8}$$

for all test functions $\varphi^v \in H^1(\Gamma[X])^3$ and $\varphi^v \in H^1(\Gamma[X])^3$, $\varphi^H \in H^1(\Gamma[X])$, and $\varphi^w \in H^1(\Gamma[X])$ with $\partial^{\bullet}\varphi^w = 0$. Here, we use the Sobolev space $H^1(\Gamma) = \{u \in L^2(\Gamma) : \nabla_{\Gamma}u \in L^2(\Gamma)\}$. This system is complemented with the initial data X^0, ν^0, H^0 and w^0 .

An alternative weak formulation of (2.8), which is similar to (2.7b)–(2.7c), but it involves the surface velocity, is based on

$$\int_{\Gamma[X]} \partial^{\bullet} w \varphi^{w} + \int_{\Gamma[X]} \nabla_{\Gamma[X]} w \cdot \nabla_{\Gamma[X]} \varphi^{w} = \int_{\Gamma[X]} F(w, \nabla_{\Gamma[X]} w) \varphi^{w} - \int_{\Gamma[X]} (\nabla_{\Gamma[X]} \cdot v) w \varphi^{w},$$

for $\varphi^w \in H^1(\Gamma[X])$ (not requiring $\partial^{\bullet} \varphi^w = 0$). Using the geometric quantities in the velocity law (2.3), using the following expression for the divergence

$$\begin{split} \nabla_{\Gamma[X]} \cdot v &= \nabla_{\Gamma[X]} \cdot (-V\nu) = -(\nabla_{\Gamma[X]}V) \cdot \nu - V(\nabla_{\Gamma[X]} \cdot \nu) \\ &= -(\nabla_{\Gamma[X]}(H - g(w)) \cdot \nu - (H - g(w))(\nabla_{\Gamma[X]} \cdot \nu), \end{split}$$

is further rewritten (into a similar form as (2.7b) and (2.7c)) as

$$\int_{\Gamma[X]} \partial^{\bullet} w \varphi^{w} + \int_{\Gamma[X]} \nabla_{\Gamma[X]} w \cdot \nabla_{\Gamma[X]} \varphi^{w} = \int_{\Gamma[X]} F_{2}(H, \nu, w, \nabla_{\Gamma[X]} H, \nabla_{\Gamma[X]} \nu, \nabla_{\Gamma[X]} w) \varphi^{w}.$$
(2.9)

Throughout the paper both the usual Euclidean scalar product for vectors and the Frobenius inner product for matrices (which equals to the Euclidean product using an arbitrary vectorisation) are denoted by a dot.

Remark 2.2. We remark here, however tempting to include, forcing terms $g(w, \nabla_{\Gamma} w)$ involving the tangential gradient of w cannot be covered by the analysis presented below. The cited stability arguments would not work for the Laplacian term for g in (2.6), or for the velocity law (2.7a).

3 Evolving finite element semi-discretization

3.1 Evolving surface finite elements

We formulate the evolving surface finite element (ESFEM) discretization for the velocity law coupled with evolution equations on the evolving surface, following the description in [24, 23], which is based on [12] and [11]. We use simplicial finite elements and continuous piecewise polynomial basis functions of degree k, as defined in [11, Section 2.5].

We triangulate the given smooth initial surface Γ^0 by an admissible family of triangulations \mathcal{T}_h of decreasing maximal element diameter h; see [14] for the notion of an admissible triangulation, which includes quasi-uniformity and shape regularity. For a momentarily fixed h, we denote by \mathbf{x}^0 the vector in \mathbb{R}^{3N} that collects all nodes p_j $(j=1,\ldots,N)$ of the initial triangulation. By piecewise polynomial interpolation of degree k, the nodal vector defines an approximate surface Γ_h^0 that interpolates Γ^0 in the nodes p_j . We will evolve the jth node in time, denoted $x_j(t)$ with $x_j(0) = p_j$, and collect the nodes at time t in a column vector

$$\mathbf{x}(t) \in \mathbb{R}^{3N}$$
.

We just write x for x(t) when the dependence on t is not important.

By piecewise polynomial interpolation on the plane reference triangle that corresponds to every curved triangle of the triangulation, the nodal vector \mathbf{x} defines a closed surface denoted by $\Gamma_h[\mathbf{x}]$. We can then define globally continuous finite element *basis functions*

$$\phi_i[\mathbf{x}]: \Gamma_h[\mathbf{x}] \to \mathbb{R}, \qquad i = 1, \dots, N,$$

which have the property that on every triangle their pullback to the reference triangle is polynomial of degree k, and which satisfy at the nodes $\phi_i[\mathbf{x}](x_j) = \Delta_{ij}$ for all $i, j = 1, \dots, N$. These functions span the finite element space on $\Gamma_h[\mathbf{x}]$,

$$S_h[\mathbf{x}] = S_h(\Gamma_h[\mathbf{x}]) = \operatorname{span}\{\phi_1[\mathbf{x}], \phi_2[\mathbf{x}], \dots, \phi_N[\mathbf{x}]\}.$$

For a finite element function $u_h \in S_h[\mathbf{x}]$, the tangential gradient $\nabla_{\Gamma_h[\mathbf{x}]} u_h$ is defined piecewise on each element.

The discrete surface at time t is parametrized by the initial discrete surface via the map $X_h(\cdot,t):\Gamma_h^0\to\Gamma_h[\mathbf{x}(t)]$ defined by

$$X_h(p_h, t) = \sum_{j=1}^{N} x_j(t) \,\phi_j[\mathbf{x}(0)](p_h), \qquad p_h \in \Gamma_h^0,$$

which has the properties that $X_h(p_j,t)=x_j(t)$ for $j=1,\ldots,N$, that $X_h(p_h,0)=p_h$ for all $p_h\in\Gamma_h^0$, and

$$\Gamma_h[\mathbf{x}(t)] = \Gamma[X_h(\cdot, t)] = \{X_h(p_h, t) : p_h \in \Gamma_h^0\}.$$

The discrete velocity $v_h(x,t) \in \mathbb{R}^3$ at a point $x = X_h(p_h,t) \in \Gamma[X_h(\cdot,t)]$ is given by

$$\partial_t X_h(p_h, t) = v_h(X_h(p_h, t), t).$$

In view of the transport property of the basis functions [14], $\frac{d}{dt} (\phi_j[\mathbf{x}(t)](X_h(p_h,t))) = 0$, the discrete velocity equals, for $x \in \Gamma_h[\mathbf{x}(t)]$,

$$v_h(x,t) = \sum_{j=1}^{N} v_j(t) \phi_j[\mathbf{x}(t)](x) \quad \text{with } v_j(t) = \dot{x}_j(t),$$

where the dot denotes the time derivative d/dt. Hence, the discrete velocity $v_h(\cdot, t)$ is in the finite element space $S_h[\mathbf{x}(t)]$, with nodal vector $\mathbf{v}(t) = \dot{\mathbf{x}}(t)$.

The discrete material derivative of a finite element function $u_h(x,t)$ with nodal values $u_j(t)$ is

$$\partial_h^{\bullet} u_h(x,t) = \frac{\mathrm{d}}{\mathrm{d}t} u_h(X_h(p_h,t)) = \sum_{j=1}^N \dot{u}_j(t) \phi_j[\mathbf{x}(t)](x) \quad \text{at} \quad x = X_h(p_h,t).$$

3.2 ESFEM spatial semi-discretizationss

Now we will describe the semi-discretization of the coupled system using both formulations of the surface PDE.

The finite element spatial semi-discretization of the weak coupled parabolic system (2.7) and (2.8) reads as follows: Find the unknown nodal vector $\mathbf{x}(t) \in \mathbb{R}^{3N}$ and the unknown finite element functions $v_h(\cdot,t) \in S_h[\mathbf{x}(t)]^3$ and $v_h(\cdot,t) \in S_h[\mathbf{x}(t)]^3$, $H_h(\cdot,t) \in S_h[\mathbf{x}(t)]$, and $w_h(\cdot,t) \in S_h[\mathbf{x}(t)]$ such that, by denoting $\alpha_h^2 = |\nabla_{\Gamma_h[\mathbf{x}]} \nu_h|^2$ and $V_h = H_h - g(w_h)$,

$$\int_{\Gamma_{h}[\mathbf{x}]} \nabla_{\Gamma_{h}[\mathbf{x}]} v_{h} \cdot \nabla_{\Gamma_{h}[\mathbf{x}]} \varphi_{h}^{v} + \int_{\Gamma_{h}[\mathbf{x}]} v_{h} \cdot \varphi_{h}^{v} = -\int_{\Gamma_{h}[\mathbf{x}]} \nabla_{\Gamma_{h}[\mathbf{x}]} (V_{h} \nu_{h}) \cdot \nabla_{\Gamma_{h}[\mathbf{x}]} \varphi_{h}^{v} - \int_{\Gamma_{h}[\mathbf{x}]} V_{h} \nu_{h} \cdot \varphi_{h}^{v}$$
(3.1a)

$$\int_{\Gamma_{h}[\mathbf{x}]} \partial_{h}^{\bullet} \nu_{h} \cdot \varphi_{h}^{\nu} + \int_{\Gamma_{h}[\mathbf{x}]} \nabla_{\Gamma_{h}[\mathbf{x}]} \nu_{h} \cdot \nabla_{\Gamma_{h}[\mathbf{x}]} \varphi_{h}^{\nu} = \int_{\Gamma_{h}[\mathbf{x}]} \alpha_{h}^{2} \nu_{h} \cdot \varphi_{h}^{\nu} - \int_{\Gamma_{h}[\mathbf{x}]} \nabla_{\Gamma_{h}[\mathbf{x}]} (g(w_{h})) \cdot \varphi_{h}^{\nu} \quad (3.1b)$$

$$\int_{\Gamma_{h}[\mathbf{x}]} \partial_{h}^{\bullet} H_{h} \varphi_{h}^{H} + \int_{\Gamma_{h}[\mathbf{x}]} \nabla_{\Gamma_{h}[\mathbf{x}]} H_{h} \cdot \nabla_{\Gamma_{h}[\mathbf{x}]} \varphi_{h}^{H} = \int_{\Gamma_{h}[\mathbf{x}]} \alpha_{h}^{2} V_{h} \varphi_{h}^{H} + \int_{\Gamma_{h}[\mathbf{x}]} \nabla_{\Gamma_{h}[\mathbf{x}]} (g(w_{h})) \cdot \nabla_{\Gamma_{h}[\mathbf{x}]} \varphi_{h}^{H},$$

(3.1c)

$$\frac{\mathrm{d}}{\mathrm{d}t} \int_{\Gamma_h[\mathbf{x}]} w_h \varphi_h^w + \int_{\Gamma_h[\mathbf{x}]} \nabla_{\Gamma_h[\mathbf{x}]} w_h \cdot \nabla_{\Gamma_h[\mathbf{x}]} \varphi_h^w = \int_{\Gamma_h[\mathbf{x}]} F(w_h, \nabla_{\Gamma_h[\mathbf{x}]} w_h) \varphi_h^w$$
(3.2)

for all $\varphi_h^v \in S_h[\mathbf{x}(t)]^3$, $\varphi_h^\nu \in S_h[\mathbf{x}(t)]^3$, $\varphi_h^H \in S_h[\mathbf{x}(t)]$, and $\varphi_h^w \in S_h[\mathbf{x}(t)]$, with the surface $\Gamma_h[\mathbf{x}(t)] = \Gamma[X_h(\cdot,t)]$ given by the differential equation

$$\partial_t X_h(p_h, t) = v_h(X_h(p_h, t), t), \qquad p_h \in \Gamma_h^0. \tag{3.3}$$

The initial values for the nodal vector \mathbf{x} are taken as the positions of the nodes of the triangulation of the given initial surface Γ^0 . The initial data for ν_h , H_h and w_h are determined by Lagrange interpolation of ν^0 , H^0 and w^0 , respectively.

Alternatively, the finite element spatial semi-discretization of the weak coupled parabolic system (2.7) and (2.9) determines the same unknown functions, but, instead of (3.2), the equations (3.1) and the ODE (3.3) are coupled to

$$\int_{\Gamma_h[\mathbf{x}]} \partial_h^{\bullet} w_h \varphi_h^w + \int_{\Gamma_h[\mathbf{x}]} \nabla_{\Gamma[X]} w_h \cdot \nabla_{\Gamma_h[\mathbf{x}]} \varphi_h^w = \int_{\Gamma_h[\mathbf{x}]} F_2(H_h, \nu_h, w_h, \nabla_{\Gamma_h[\mathbf{x}]} H_h, \nabla_{\Gamma_h[\mathbf{x}]} \nu_h, \nabla_{\Gamma_h[\mathbf{x}]} w_h) \varphi_h^w,$$
(3.4)

for all $\varphi_h^w \in S_h[\mathbf{x}(t)]$.

In the above approaches, the discretization of the evolution equations for ν , H and w is done in the usual way of evolving surface finite elements. The velocity law (2.3) is enforced by a Ritz projection to the finite element space on $\Gamma_h[\mathbf{x}]$. Taking instead just the finite element interpolation or L^2 projection does not appear to be sufficient for a convergence analysis (but in our experience both work well in practice). Note that the finite element functions ν_h and H_h are *not* the normal vector and the mean curvature of the discrete surface $\Gamma_h[\mathbf{x}(t)]$.

3.3 Matrix-vector formulations

We collect the nodal values in column vectors $\mathbf{v} = (v_j) \in \mathbb{R}^{3N}$, $\mathbf{n} = (\nu_j) \in \mathbb{R}^{3N}$, $\mathbf{H} = (H_j) \in \mathbb{R}^N$ and $\mathbf{w} = (w_j) \in \mathbb{R}^N$.

We define the surface-dependent mass matrix $\mathbf{M}(\mathbf{x})$ and stiffness matrix $\mathbf{A}(\mathbf{x})$ on the surface determined by the nodal vector \mathbf{x} :

$$\mathbf{M}(\mathbf{x})|_{ij} = \int_{\Gamma_h[\mathbf{x}]} \phi_i[\mathbf{x}] \phi_j[\mathbf{x}],$$

$$\mathbf{A}(\mathbf{x})|_{ij} = \int_{\Gamma_h[\mathbf{x}]} \nabla_{\Gamma_h[\mathbf{x}]} \phi_i[\mathbf{x}] \cdot \nabla_{\Gamma_h[\mathbf{x}]} \phi_j[\mathbf{x}],$$

$$i, j = 1, \dots, N,$$

with the finite element nodal basis functions $\phi_j[\mathbf{x}] \in S_h[\mathbf{x}]$. We define the nonlinear functions $\mathbf{f}(\mathbf{x}, \mathbf{n}, \mathbf{H}, \mathbf{w}) \in \mathbb{R}^{4N}$, $\mathbf{g}(\mathbf{x}, \mathbf{n}, \mathbf{H}, \mathbf{w}) \in \mathbb{R}^{3N}$ and $\mathbf{F}(\mathbf{x}, \mathbf{w}) \in \mathbb{R}^N$, where

$$\mathbf{f}(\mathbf{x},\mathbf{n},\mathbf{H},\mathbf{w}) = \left(egin{array}{c} \mathbf{f}_1(\mathbf{x},\mathbf{n},\mathbf{H},\mathbf{w}) \ \mathbf{f}_2(\mathbf{x},\mathbf{n},\mathbf{H},\mathbf{w}) \end{array}
ight)$$

with $\mathbf{f}_1(\mathbf{x}, \mathbf{n}, \mathbf{H}, \mathbf{w}) \in \mathbb{R}^{3N}$ and $\mathbf{f}_2(\mathbf{x}, \mathbf{n}, \mathbf{H}, \mathbf{w}) \in \mathbb{R}^N$ given by, with the notations $\alpha_h^2 = |\nabla_{\Gamma_h[\mathbf{x}]} \nu_h|^2$ and $V_h = H_h - g(w_h)$,

$$\mathbf{f}_{1}(\mathbf{x}, \mathbf{n}, \mathbf{H}, \mathbf{w})|_{j+(\ell-1)N} = \int_{\Gamma_{h}[\mathbf{x}]} \alpha_{h}^{2} (\nu_{h})_{\ell} \phi_{j}[\mathbf{x}] - \int_{\Gamma_{h}[\mathbf{x}]} \left(\nabla_{\Gamma_{h}[\mathbf{x}]} (g(w_{h}))\right)_{\ell} \cdot \phi_{j}[\mathbf{x}],$$

$$\mathbf{f}_{2}(\mathbf{x}, \mathbf{n}, \mathbf{H}, \mathbf{w})|_{j} = \int_{\Gamma_{h}[\mathbf{x}]} \alpha_{h}^{2} V_{h} \phi_{j}[\mathbf{x}] + \int_{\Gamma_{h}[\mathbf{x}]} \nabla_{\Gamma_{h}[\mathbf{x}]} (g(w_{h})) \cdot \nabla_{\Gamma_{h}[\mathbf{x}]} \phi_{j}[\mathbf{x}],$$

$$\mathbf{g}(\mathbf{x}, \mathbf{n}, \mathbf{H}, \mathbf{w})|_{j+(\ell-1)N} = -\int_{\Gamma_{h}[\mathbf{x}]} V_{h} (\nu_{h})_{\ell} \phi_{j}[\mathbf{x}] - \int_{\Gamma_{h}[\mathbf{x}]} \nabla_{\Gamma_{h}[\mathbf{x}]} \left(V_{h} (\nu_{h})_{\ell}\right) \cdot \nabla_{\Gamma_{h}[\mathbf{x}]} \phi_{j}[\mathbf{x}],$$

$$\mathbf{F}(\mathbf{x}, \mathbf{w})|_{j} = \int_{\Gamma_{h}[\mathbf{x}]} F(w_{h}, \nabla_{\Gamma_{h}[\mathbf{x}]} w_{h}) \phi_{j}[\mathbf{x}]$$

for j = 1, ..., N and $\ell = 1, 2, 3$.

We further let, for $d \in \mathbb{N}$ (with the identity matrices $I_d \in \mathbb{R}^{d \times d}$)

$$\mathbf{M}^{[d]}(\mathbf{x}) = I_d \otimes \mathbf{M}(\mathbf{x}), \qquad \mathbf{A}^{[d]}(\mathbf{x}) = I_d \otimes \mathbf{A}(\mathbf{x}), \qquad \mathbf{K}^{[d]}(\mathbf{x}) = I_d \otimes (\mathbf{M}(\mathbf{x}) + \mathbf{A}(\mathbf{x})).$$

When no confusion can arise, we will write $\mathbf{M}(\mathbf{x})$ for $\mathbf{M}^{[d]}(\mathbf{x})$, $\mathbf{A}(\mathbf{x})$ for $\mathbf{A}^{[d]}(\mathbf{x})$, and $\mathbf{K}(\mathbf{x})$ for $\mathbf{K}^{[d]}(\mathbf{x})$.

Then, the equations (3.1) and (3.2) with (3.3), denoting

$$\mathbf{u} = \left(egin{array}{c} \mathbf{n} \\ \mathbf{H} \end{array}
ight) \in \mathbb{R}^{4N},$$

can be written in the following matrix-vector form:

$$\mathbf{K}^{[3]}(\mathbf{x})\mathbf{v} = \mathbf{g}(\mathbf{x}, \mathbf{u}, \mathbf{w}),$$

$$\mathbf{M}^{[4]}(\mathbf{x})\dot{\mathbf{u}} + \mathbf{A}^{[4]}(\mathbf{x})\mathbf{u} = \mathbf{f}(\mathbf{x}, \mathbf{u}, \mathbf{w}),$$

$$\frac{d}{dt}(\mathbf{M}(\mathbf{x})\mathbf{w}) + \mathbf{A}(\mathbf{x})\mathbf{w} = \mathbf{F}(\mathbf{x}, \mathbf{w})$$

$$\dot{\mathbf{x}} = \mathbf{v}$$
(3.5)

Similarly, the equations (3.1) and (3.4) with (3.3), denoting

$$\mathbf{u} = \left(egin{array}{c} \mathbf{n} \ \mathbf{H} \ \mathbf{w} \end{array}
ight) \in \mathbb{R}^{5N},$$

can be written in the matrix-vector formulation, where $\mathcal{F} = (\mathbf{f}_1, \mathbf{f}_2, \mathbf{F}_2)^T$ with \mathbf{f}_i same as before and with \mathbf{F}_2 being the vector corresponding to the right-hand side of (3.4),

$$\mathbf{K}^{[3]}(\mathbf{x})\mathbf{v} = \mathbf{g}(\mathbf{x}, \mathbf{u}),$$

$$\mathbf{M}^{[5]}(\mathbf{x})\dot{\mathbf{u}} + \mathbf{A}^{[5]}(\mathbf{x})\mathbf{u} = \mathcal{F}(\mathbf{x}, \mathbf{u}),$$

$$\dot{\mathbf{x}} = \mathbf{v}.$$
(3.6)

The system (3.6) for *forced* mean curvature flow is formally the same as the matrix–vector form of the coupled system for *non-forced* mean curvature flow, derived in [23], cf. (3.4)–(3.5) therein.

3.4 Lifts

As in [24] and [23, Section 3.4], we compare functions on the exact surface $\Gamma[X(\cdot,t)]$ with functions on the discrete surface $\Gamma_h[\mathbf{x}(t)]$, via functions on the interpolated surface $\Gamma_h[\mathbf{x}^*(t)]$, where $\mathbf{x}^*(t)$ denotes the nodal vector collecting the grid points $x_j^*(t) = X(p_j,t)$ on the exact surface, where p_j are the nodes of the discrete initial triangulation Γ_h^0 .

Any finite element function w_h on the discrete surface, with nodal values w_j , is associated with a finite element function \widehat{w}_h on the interpolated surface Γ_h^* with the exact same nodal values. This can be further lifted to a function on the exact surface by using the *lift operator* l, mapping a function on the interpolated surface Γ_h^* to a function on the exact surface Γ , provided that they are sufficiently close, see [12, 11].

Then the composed lift L maps finite element functions on the discrete surface $\Gamma_h[\mathbf{x}(t)]$ to functions on the exact surface $\Gamma[X(\cdot,t)]$ via the interpolated surface $\Gamma_h[\mathbf{x}^*(t)]$ is denoted by

$$w_h^L = (\widehat{w}_h)^l$$
.

4 Convergence of the semi-discretizations

We are now in the position to formulate the first main result of this paper, which yields optimalorder error bounds for the finite element semi-discretization (using finite elements of polynomial degree $k \ge 2$) (3.1), and (3.2) or (3.4), with (3.3) of the system for forced mean curvature equations (2.7), and one of the weak formulations (2.8) or (2.9) for the surface PDE, with the ODE (2.1) for the positions. We introduce the notation

$$x_h^L(x,t) = X_h^L(p,t) \in \Gamma_h[\mathbf{x}(t)]$$
 for $x = X(p,t) \in \Gamma[X(\cdot,t)].$

Theorem 4.1. Consider the space discretizations (3.5) or (3.6) (in their matrix–vector form) of the coupled *forced* mean curvature flow problem (2.7), and (2.8) or (2.9), with (2.1), using evolving surface finite elements of polynomial degree $k \geq 2$. Suppose that the problem admits an exact solution (X, v, ν, H, w) that is sufficiently smooth on the time interval $t \in [0, T]$, and that the flow map $X(\cdot, t) : \Gamma^0 \to \Gamma[X] \subset \mathbb{R}^3$ is non-degenerate so that $\Gamma[X]$ is a regular surface on the time interval $t \in [0, T]$.

Then for both formulations, there exists a constant $h_0 > 0$ such that for all mesh sizes $h \le h_0$ the following error bounds for the lifts of the discrete position, velocity, normal vector and mean curvature hold over the exact surface $\Gamma(t) = \Gamma[X(\cdot,t)]$ for $0 \le t \le T$:

$$||x_h^L(\cdot,t) - \mathrm{id}_{\Gamma(t)}||_{H^1(\Gamma(t))^3} \le Ch^k, ||v_h^L(\cdot,t) - v(\cdot,t)||_{H^1(\Gamma(t))^3} \le Ch^k, ||v_h^L(\cdot,t) - v(\cdot,t)||_{H^1(\Gamma(t))^3} \le Ch^k, ||H_h^L(\cdot,t) - H(\cdot,t)||_{H^1(\Gamma(t))} \le Ch^k, ||w_h^L(\cdot,t) - w(\cdot,t)||_{H^1(\Gamma(t))} \le Ch^k,$$

and also

$$||X_h^l(\cdot,t) - X(\cdot,t)||_{H^1(\Gamma_0)^3} \le Ch^k,$$

where the constant C is independent of h and t, but depends on bounds of higher derivatives of the solution (X, v, ν, H, w) of the forced mean curvature flow and on the length T of the time interval.

Sufficient regularity assumptions are the following: with bounds that are uniform in $t \in [0,T]$, we assume $X(\cdot,t) \in H^{k+1}(\Gamma^0)$, $v(\cdot,t) \in H^{k+1}(\Gamma(X(\cdot,t)))^3$, and for $u=(\nu,H,w)$ we have $u(\cdot,t)$, $\partial^{\bullet}u(\cdot,t) \in W^{k+1,\infty}(\Gamma(X(\cdot,t)))^5$.

The proof of Theorem 4.1 for the semi-discretisation (3.6) follows from the stability bound [23, Proposition 7.1], combined with consistency of the numerical scheme, which are shown exactly as in [23, Lemma 8.1].

Remark 4.2. For the semi-discretisation (3.5) a stability proof can be obtained by combining the stability proofs of our previous works [24] and [23]. The stability of the scheme is obtained by combining the results of [24, Proposition 6.1] (in particular part (A)) for the surface PDE, and of [23, Proposition 7.1] for the velocity law and for the geometric quantities. Numerical experiments presented in Section 7 demonstrate that semi-discrete error estimates, similar to those in Theorem ??, also hold for the scheme (5.3).

5 Linearly implicit full discretization

For the time discretization of the system of ordinary differential equations of Section 3.3 we use a q-step linearly implicit backward difference formula (BDF) with $q \le 5$. For a step size $\tau > 0$, and with $t_n = n\tau \le T$, let us introduce, for $n \ge q$,

the discrete time derivative
$$\dot{\mathbf{u}}^n = \frac{1}{\tau} \sum_{j=0}^q \delta_j \mathbf{u}^{n-j}$$
, and (5.1)

the extrapolated value
$$\widetilde{\mathbf{u}}^n = \sum_{j=0}^{q-1} \gamma_j \mathbf{u}^{n-1-j},$$
 (5.2)

where the coefficients are given by $\delta(\zeta) = \sum_{j=0}^q \delta_j \zeta^j = \sum_{\ell=1}^q \frac{1}{\ell} (1-\zeta)^\ell$ and $\gamma(\zeta) = \sum_{j=0}^{q-1} \gamma_j \zeta^j = (1-(1-\zeta)^q)/\zeta$, respectively.

We determine the approximations \mathbf{x}^n to $\mathbf{x}(t_n)$, \mathbf{v}^n to $\mathbf{v}(t_n)$, \mathbf{u}^n to $\mathbf{u}(t_n)$, and \mathbf{w}^n to $\mathbf{w}(t_n)$ (only if not already collected into \mathbf{u}) by the linearly implicit BDF discretisation of both systems (3.5) and (3.6).

For (3.5) we obtain

$$\mathbf{K}(\widetilde{\mathbf{x}}^{n})\mathbf{v}^{n} = \mathbf{g}(\widetilde{\mathbf{x}}^{n}, \widetilde{\mathbf{u}}^{n}, \widetilde{\mathbf{w}}^{n}),$$

$$\mathbf{M}(\widetilde{\mathbf{x}}^{n})\dot{\mathbf{u}}^{n} + \mathbf{A}(\widetilde{\mathbf{x}}^{n})\mathbf{u}^{n} = \mathbf{f}(\widetilde{\mathbf{x}}^{n}, \widetilde{\mathbf{u}}^{n}, \widetilde{\mathbf{w}}^{n}),$$

$$\frac{1}{\tau} \sum_{j=0}^{q} \Delta_{j} \mathbf{M}(\widetilde{\mathbf{x}}^{n-j})\mathbf{w}^{n-j} + \mathbf{A}(\widetilde{\mathbf{x}}^{n})\mathbf{w}^{n} = \mathbf{F}(\widetilde{\mathbf{x}}^{n}, \widetilde{\mathbf{w}}^{n}),$$

$$\dot{\mathbf{x}}^{n} = \mathbf{v}^{n}.$$
(5.3)

While for (3.6) we obtain

$$\mathbf{K}(\widetilde{\mathbf{x}}^{n})\mathbf{v}^{n} = \mathbf{g}(\widetilde{\mathbf{x}}^{n}, \widetilde{\mathbf{u}}^{n}),$$

$$\mathbf{M}(\widetilde{\mathbf{x}}^{n})\dot{\mathbf{u}}^{n} + \mathbf{A}(\widetilde{\mathbf{x}}^{n})\mathbf{u}^{n} = \boldsymbol{\mathcal{F}}(\widetilde{\mathbf{x}}^{n}, \widetilde{\mathbf{u}}^{n}),$$

$$\dot{\mathbf{x}}^{n} = \mathbf{v}^{n}.$$
(5.4)

The starting values \mathbf{x}^i , \mathbf{u}^i , and, in case of (5.3), \mathbf{w}^i , for $i=0,\ldots,q-1$, are assumed to be given. They can be precomputed using either a lower order method with smaller step sizes or an implicit Runge–Kutta method.

The classical BDF method is known to be zero-stable for $q \le 6$ and to have order q; see [21, Chapter V]. This order is retained by the linearly implicit variant (for $q \le 5$) using the above coefficients γ_i ; cf. [1].

From the vectors $\mathbf{x}^n = (x_j^n)$, $\mathbf{v}^n = (v_j^n)$, and $\mathbf{u}^n = (u_j^n)$ with $u_j^n = (\nu_j^n, H_j^n) \in \mathbb{R}^3 \times \mathbb{R}$ and $\mathbf{w}^n = (w_j^n)$, or $\mathbf{u}^n = (u_j^n)$ with $u_j^n = (\nu_j^n, H_j^n, w_j^n) \in \mathbb{R}^3 \times \mathbb{R} \times \mathbb{R}$ we obtain approximations to their respective variables as finite element functions whose nodal values are collected in these vectors.

6 Convergence of the full discretization

We are now in the position to formulate the second main result of this paper, which yields optimal-order error bounds for the combined ESFEM-BDF full discretizations (5.4) of the coupled forced mean curvature flow problem (2.7) coupled to the weak form (2.9) of the surface PDE, with (2.1), for finite elements of polynomial degree $k \geq 2$ and BDF methods of order 2 < q < 5.

Theorem 6.1. Consider the ESFEM-BDF full discretizations (5.4) of the coupled forced mean curvature flow problem (2.7) and (2.9), with (2.1), using evolving surface finite elements of polynomial degree $k \geq 2$ and linearly implicit BDF time discretization of order q with $2 \leq q \leq 5$. Suppose that the *forced* mean curvature flow problem admits an exact solution (X, v, v, H, w) that is sufficiently smooth on the time interval $t \in [0, T]$, and that the flow map $X(\cdot, t) : \Gamma^0 \to \Gamma[X] \subset \mathbb{R}^3$ is non-degenerate so that $\Gamma[X]$ is a regular surface on the time interval $t \in [0, T]$. Assume that the starting values are sufficiently accurate in the H^1 norm at time $t_i = i\tau$ for $i = 0, \ldots, q-1$.

Then for both method (5.4), there exist $h_0>0$ and $\tau_0>0$ such that for all mesh sizes $h\leq h_0$ and time step sizes $\tau\leq\tau_0$ satisfying the step size restriction

$$\tau < C_0 h \tag{6.1}$$

(where $C_0 > 0$ can be chosen arbitrarily), the following error bounds for the lifts of the discrete position, velocity, normal vector and mean curvature hold over the exact surface $\Gamma(t_n) =$

$$\begin{split} \Gamma[X(\cdot,t_n)] \text{ at time } t_n &= n\tau \leq T; \\ & \| (x_h^n)^L - \mathrm{id}_{\Gamma(t_n)} \|_{H^1(\Gamma(t_n))^3} \leq C(h^k + \tau^q), \\ & \| (v_h^n)^L - v(\cdot,t_n) \|_{H^1(\Gamma(t_n))^3} \leq C(h^k + \tau^q), \\ & \| (\nu_h^n)^L - v(\cdot,t_n) \|_{H^1(\Gamma(t_n))^3} \leq C(h^k + \tau^q), \\ & \| (H_h^n)^L - H(\cdot,t_n) \|_{H^1(\Gamma(t_n))} \leq C(h^k + \tau^q), \\ & \| (w_h^n)^L - w(\cdot,t_n) \|_{H^1(\Gamma(t_n))} \leq C(h^k + \tau^q), \end{split}$$

and also

$$||(X_h^n)^l - X(\cdot, t_n)||_{H^1(\Gamma_0)^3} \le C(h^k + \tau^q),$$

where the constant C is independent of h, τ and n with $n\tau \leq T$, but depends on bounds of higher derivatives of the solution (X, v, ν, H, w) of the forced mean curvature flow problem, on the length T of the time interval, and on C_0 .

Sufficient regularity assumptions are the following: uniformly in $t \in [0,T]$ and for $j=1,\ldots,q+1$,

$$\begin{split} X(\cdot,t) \in H^{k+1}(\Gamma^0)^3, \ \partial_t^j X(\cdot,t) \in H^1(\Gamma^0)^3, \\ v(\cdot,t) \in H^{k+1}(\Gamma(X(\cdot,t)))^3, \ \partial^{\bullet j} v(\cdot,t) \in H^2(\Gamma(X(\cdot,t)))^3, \end{split}$$
 for $u = (\nu,H,w), \quad u(\cdot,t), \partial^{\bullet} u(\cdot,t) \in W^{k+1,\infty}(\Gamma(X(\cdot,t)))^5, \\ \partial^{\bullet j} u(\cdot,t) \in H^2(\Gamma(X(\cdot,t)))^5. \end{split}$

For the starting values, sufficient approximation conditions are the following: for $i = 0, \dots, q-1$,

$$\|(x_h^i)^L - \mathrm{id}_{\Gamma(t_i)}\|_{H^1(\Gamma(t_i))^3} \le C(h^k + \tau^q),$$
 for $u = (\nu, H, w), \qquad \|(u_h^i)^L - u(\cdot, t_i)\|_{H^1(\Gamma(t_i))^3} \le C(h^k + \tau^q),$

and in addition, for $i = 1, \dots, q-1$,

$$\tau^{1/2} \left\| \frac{1}{\tau} (X_h^i - X_h^{i-1})^l - \frac{1}{\tau} (X(\cdot, t_i) - X(\cdot, t_{i-1})) \right\|_{H^1(\Gamma_0)^3} \le C(h^k + \tau^q).$$

The proof of Theorem 6.1 for the full discretisation (5.4) directly follows from the error analysis presented in [23], since (5.4) is verbatim to the matrix-vector form of mean curvature flow in [23, equation (5.1)], (recalling that here $\mathbf{u} = (\mathbf{n}, \mathbf{H}, \mathbf{w})^T$).

A similar convergence result holds for the linearly implicit backward Euler method (q = 1), which requires a slightly different direct proof due to some technical tools in the stability analysis, see [23].

Remark 6.2. For the other algorithm (5.3), a fully discrete error estimate can be obtained by combining the stability results for the coupled mean curvature flow, [23, Proposition 10.1], with the extension of the stability analysis for the surface PDE [25, Proposition 6.1] (via energy estimates obtained by testing with \dot{e}^n). We note here that, this extension, in particular the analogous steps to part (iv) in [23, Proposition 10.1], is possibly lengthy and rather nontrivial. Numerical experiments presented in Section 7 demonstrate that fully discrete error estimates, similar to those in Theorem 6.1, also hold for the scheme (5.3).

7 Numerical experiments

We present numerical experiments for the forced mean curvature flow, using both (5.3) and (5.4). For our numerical experiments we consider the problem coupling forced mean curvature flow (with a new parameter $\varepsilon > 0$) of the surface $\Gamma(X(\cdot,t))$, together with evolution equations for its normal vector ν and mean curvature H, where the forcing is given through the solution w of a reaction–diffusion problem on the surface:

$$\partial^{\bullet} w = -w(\nabla_{\Gamma[X]} \cdot v) + \Delta_{\Gamma[X]} w + f(w, \nabla_{\Gamma[X]} w) + \varrho_{1},$$

$$v = -\varepsilon H \nu + g(w) \nu + \varrho_{2},$$

$$\partial^{\bullet} \nu = \varepsilon \Delta_{\Gamma[X]} \nu + \varepsilon |A|^{2} \nu - \nabla_{\Gamma[X]} (g(w)) + \varrho_{3},$$

$$\partial^{\bullet} H = \varepsilon \Delta_{\Gamma[X]} H + \varepsilon |A|^{2} H - \Delta_{\Gamma[X]} (g(w)) - |A|^{2} g(w) + \varrho_{4},$$

$$\partial_{t} X = v,$$

$$(7.1)$$

where the inhomogeneities ϱ_i are scalar or vector valued functions on $\mathbb{R}^3 \times [0, T]$, to be specified later on.

We used this problem to perform:

- A convergence order experiment for the algorithm (5.4), in order to illustrate our theoretical results of Theorem 4.1 and 6.1.
- A convergence order experiment for algorithm (5.3), illustrating Theorem 4.1 and Remark 6.2.
- An experiment, using algorithm (5.4), for a tumour growth model from [2, Section 5], where one component of a reaction—diffusion surface PDE system forces the mean curvature flow motion of the surface. This experiment allows a direct comparison on the same problem with other methods published in the literature.

7.1 Convergence experiments

In order to illustrate the convergence results of Theorem 4.1 and 6.1, we have computed the errors between the numerical and exact solutions of the system (7.1), where the forcing is set to be $g(w) = \frac{1}{2}w^2$, and $\epsilon = 1$. The reaction therm in the PDE is $f(w, \nabla_{\Gamma[X]}w) = w^2$. The inhomogeneities ϱ_i are chosen such that the exact solution is X(q,t) = R(t)q, with q on the initial surface Γ_0 , the sphere with radius R_0 , and $w(x,t) = e^{-t}x_1x_2$, for all $x \in \Gamma[X]$ and $0 \le t \le T$. The function R satisfies the logistic differential equation:

$$\frac{\mathrm{d}R(t)}{\mathrm{d}t} = \left(1 - \frac{R(t)}{R_1}\right)R(t), \qquad t \in [0, T],$$

$$R(0) = R_0,$$

with $R_1 \ge R_0$, i.e. the exact evolving surface $\Gamma[X(\cdot,t)]$ is a sphere with radius $R(t) = R_0R_1(R_0(1-e^{-t})+R_1e^{-t})^{-1}$.

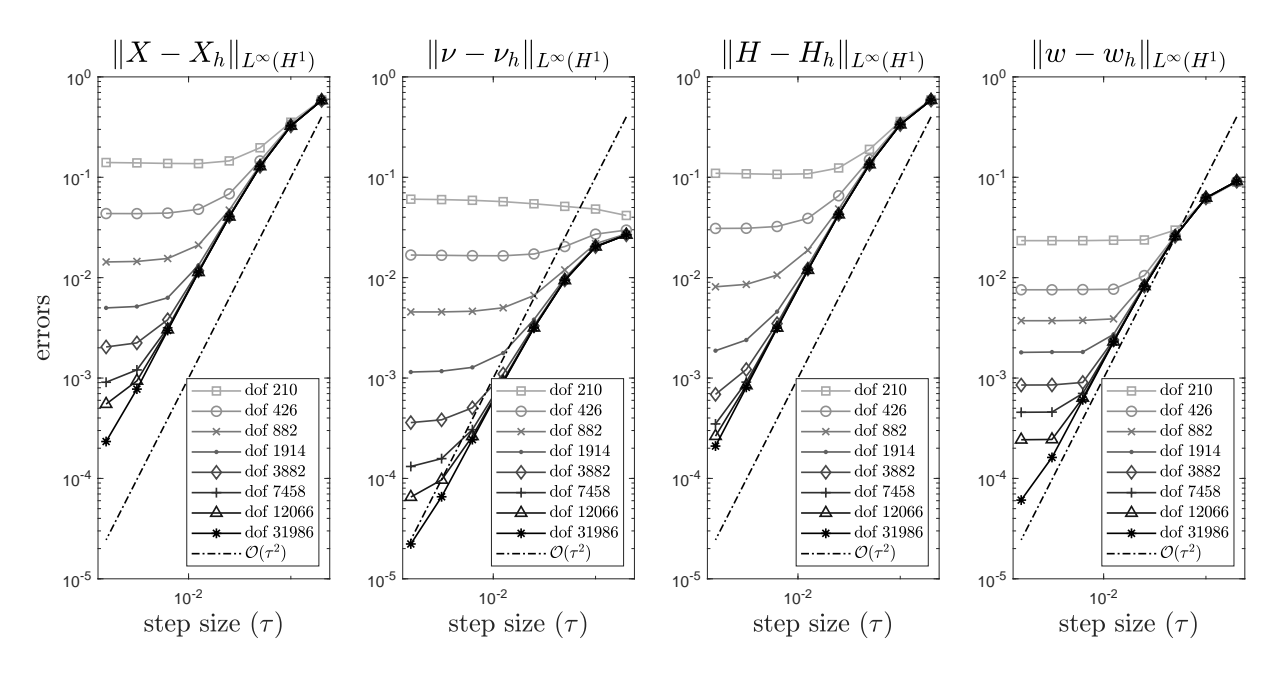


Figure 1: Temporal convergence of the algorithm (5.4) for forced MCF with $g(w) = \frac{1}{2}w^2$, using BDF2 / quadratic SFEM.

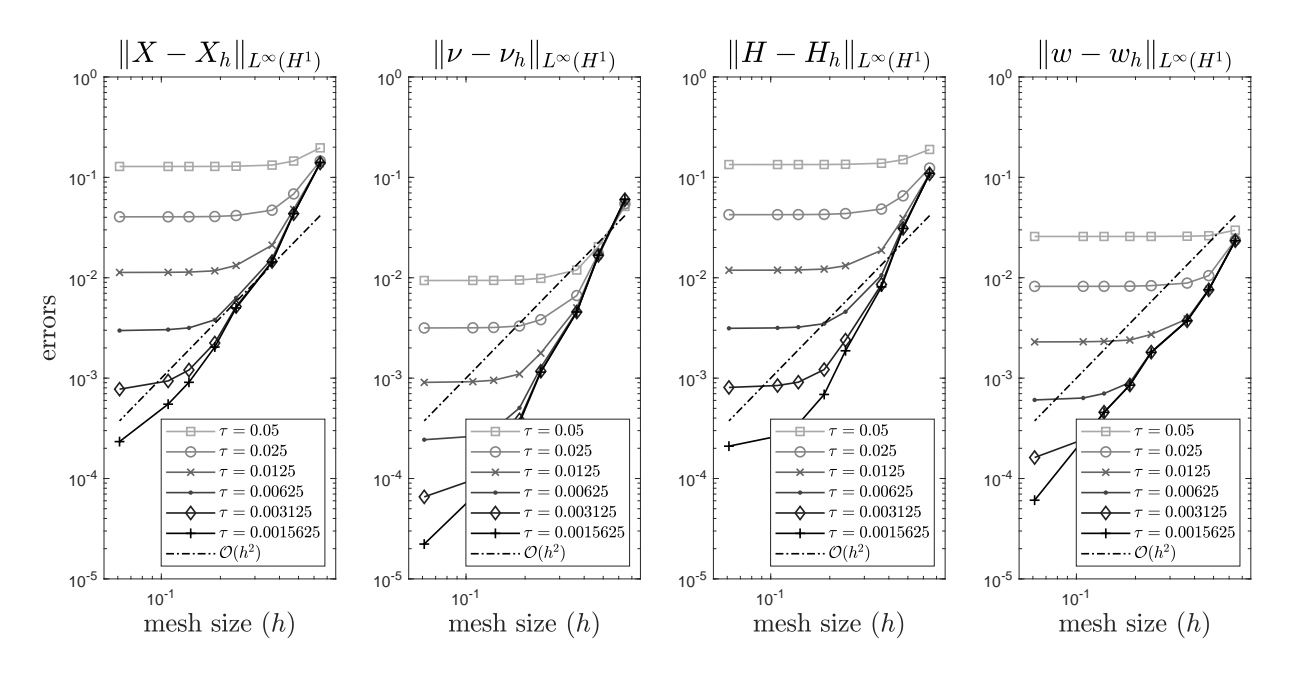


Figure 2: Spatial convergence of the algorithm (5.4) for forced MCF with $g(w)=\frac{1}{2}w^2$, using BDF2 / quadratic SFEM.

Using the algorithm in (5.4) with 2-step BDF method and quadratic evolving surface FEM, we computed approximations to forced mean curvature flow, using $R_0 = 1$ and $R_1 = 2$, until time T = 1. For our computations we used a sequence of time step sizes $\tau_k = \tau_{k-1}/2$ with $\tau_0 = 0.2$, and a sequence of initial meshes of mesh widths $h_k \approx 2^{-1/2}h_{k-1}$ with $h_0 \approx 0.5$. The numerical experiments suggest that the step size restriction (6.1) is not required in practice.

In Figure 1 and 2 we report the errors between the numerical and exact solution for all four variables, i.e. the surface error, the errors in the dynamic variables ν and H, and the error in the PDE variable w. The logarithmic plots show the $L^{\infty}(H^1)$ norm errors against the time step size τ in Figure 1, and against the mesh width h in Figure 2. The lines marked with different symbols correspond to different mesh refinements and to different time step sizes in Figure 1 and 2, respectively.

In Figure 1 we can observe two regions: a region where the temporal discretisation error dominates, matching to the $O(\tau^2)$ order of convergence of our theoretical results, and a region, with small time step sizes, where the spatial discretization error dominates (the error curves flatten out). For Figure 2, the same description applies, but with reversed roles.

Both the temporal and spatial convergence, as shown by Figures 1 and 2, respectively, are in agreement with the theoretical convergence results of Theorem 4.1 and 6.1 (note the reference lines).

We have performed the same convergence experiments using algorithm (5.3), which, in view of Theorem 4.1, Remarks 4.2 and 6.2, and the stability and convergence results previous works [26, 24, 25, 23], should also have the same convergence properties as the algorithm (5.4). As Figures (3) and (4) (created analogously as Figure 1 and 2) suggest this is indeed the case.

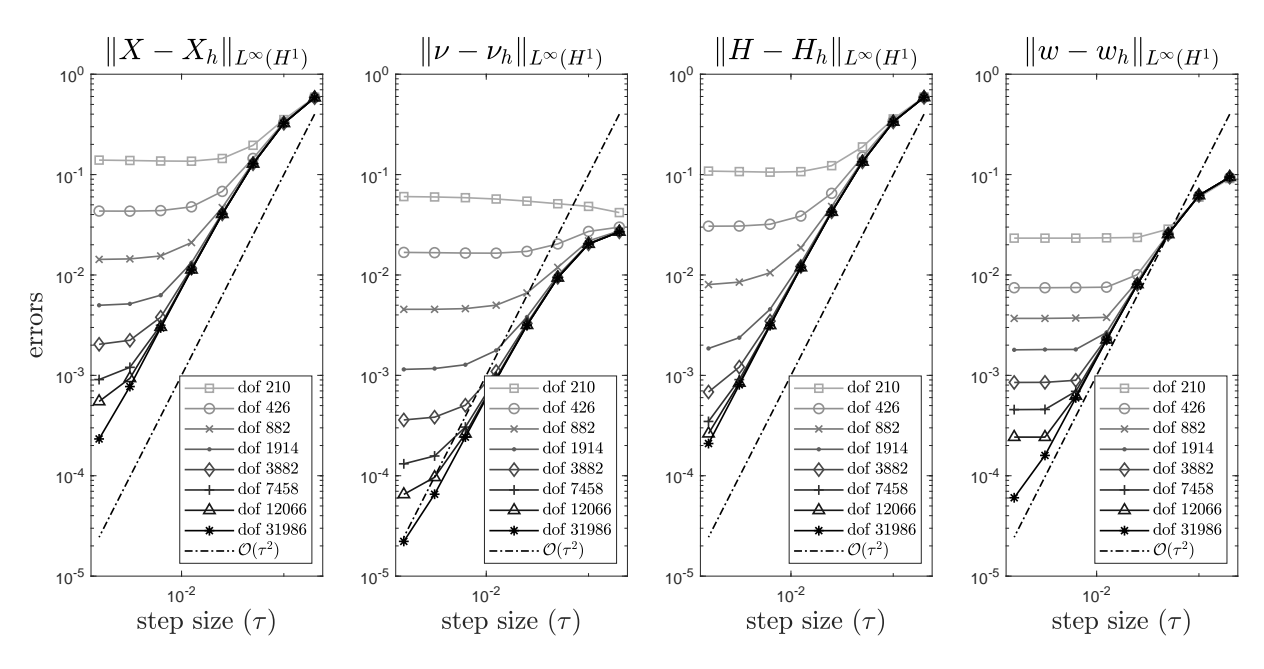


Figure 3: Temporal convergence of the algorithm (5.3) for forced MCF with $g(w)=\frac{1}{2}w^2$, using BDF2 / quadratic SFEM.

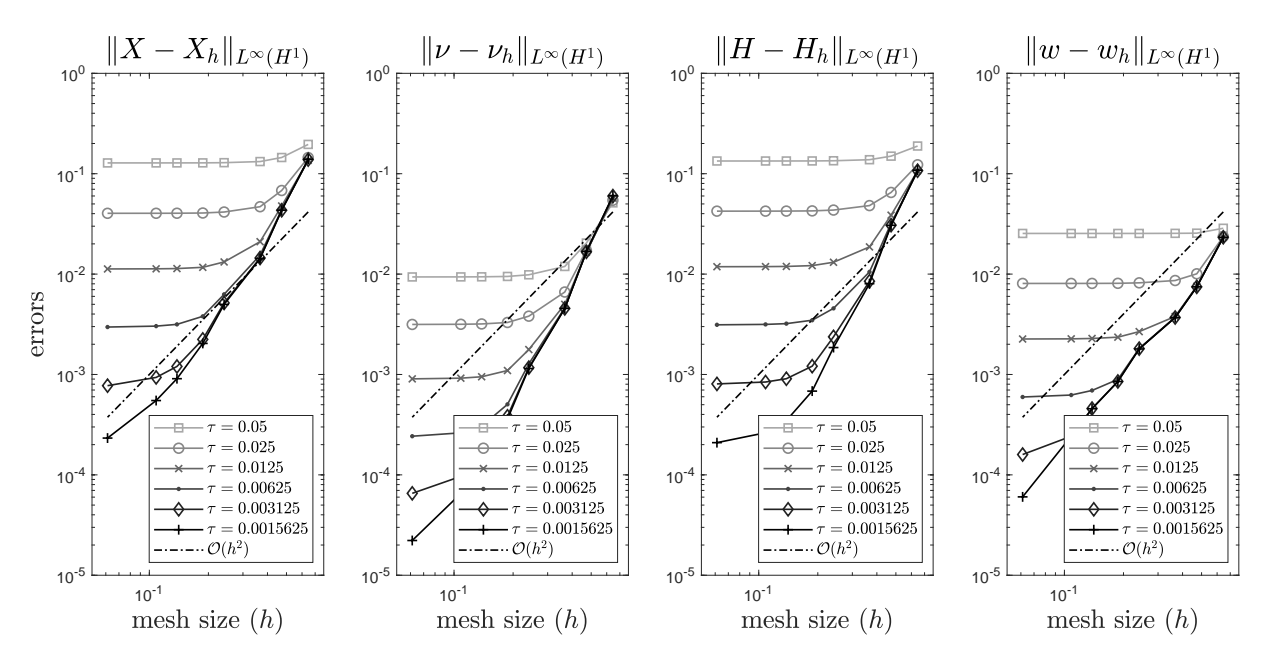


Figure 4: Spatial convergence of the algorithm (5.3) for forced MCF with $g(w) = \frac{1}{2}w^2$, using BDF2 / quadratic SFEM.

7.2 Tumour growth

We performed numerical experiments on a well-known model for forced mean curvature flow from [2, Section 5]: The problem (7.1), with vector valued unknown $w = (w_1, w_2)$ and with a small parameter $\varepsilon = 0.01$, models solid tumour growth, for further details we refer to [7, 8, 6] and [2]. Our results can be compared to those in these references, in particularly with those in [2].

The surface PDE system for $w=(w_1,w_2)$ describes the activator-depleted kinetics, and has diffusivity constants 1 and d=10 for w_1 and w_2 , respectively. The reaction term is given by, with $\gamma>0$,

$$f(w) = f(w_1, w_2) = \begin{pmatrix} \gamma(a - w_1 + w_1^2 w_2) \\ \gamma(b - w_1^2 w_2) \end{pmatrix},$$

while in the velocity law the non-linearity is given by

$$g(w) = g(w_1, w_2) = \delta w_1.$$

The parameters are chosen exactly as in [2, Table 5]: d=10, a=0.1, b=0.9, $\delta=0.1$, and $\epsilon=0.01$. The parameter γ will be varied for different experiments.

The initial data for all of the presented experiments are obtained (exactly as in [2, Section 4.1.1 and Figure 8]) by integrating the reaction-diffusion system on the fixed unit sphere over the time interval [0,5], with small random perturbations of the steady state $w_1 = a + b$ and $w_2 = b/(a+b)^2$ as initial data. Further initial values (for $i=1,\ldots,q-1$) for high-order BDF methods are computed using a cascade of steps performed by the corresponding lower order methods.

To mitigate the stiffness of the non-linear term the linear part of f(w) is handled fully implicitly, while the non-linear parts of f, and the velocity law as well, are treated linearly implicitly using the extrapolation (5.2).

In Figure 5 and 6 we report on the evolution of the surface (and the approximated mean curvature and normal vector) and the component w_1 for parameters $\gamma=30$ and $\gamma=300$, respectively, at different times over the time interval [5,8]. Figure 5 and 6 we present the surface evolution and the component w_1 of the surface PDE system (left-hand side columns) and the computed mean curvature H_h and normal vector ν_h (right-hand side columns) at times t=5,6,7,8 (the rows from top to bottom), on a mesh with 3882 nodes and time step size $\tau=0.0015625$. In particular the top rows show the initial data where the surface evolution is started. The obtained results for the surface evolution and the reaction–diffusion PDE system (left columns) match nicely (note the random effects in generating initial data) to previously reported results.

Acknowledgement

The work of Balázs Kovács and Christian Lubich is supported by Deutsche Forschungsgemeinschaft, SFB 1173. The work of Buyang Li is partially supported by an internal grant (Project ZZKQ) of The Hong Kong Polytechnic University.

References

- [1] G. Akrivis and C. Lubich. Fully implicit, linearly implicit and implicit–explicit backward difference formulae for quasi-linear parabolic equations. *Numer. Math.*, 131(4):713–735, 2015.
- [2] R. Barreira, C. M. Elliott, and A. Madzvamuse. The surface finite element method for pattern formation on evolving biological surfaces. *J. Math. Biol.*, 63(6):1095–1119, 2011.
- [3] J. Barrett, K. Deckelnick, and V. Styles. Numerical analysis for a system coupling curve evolution to reaction diffusion on the curve. *SIAM J. Numer. Anal.*, 55(2):1080–1100, 2017.
- [4] J. Barrett, H. Garcke, and R. Nürnberg. On the parametric finite element approximation of evolving hypersurfaces in \mathbb{R}^3 . *J. Comput. Phys.*, 227(9):4281–4307, 2008.
- [5] J. Barrett, H. Garcke, and R. Nürnberg. Parametric finite element approximations of curvature driven interface evolutions. *arXiv:1903.09462v1*, 2019.
- [6] M. Chaplain, M. Ganesh, and I. Graham. Spatio-temporal pattern formation on spherical surfaces: numerical simulation and application to solid tumour growth. *J. Math. Biol.*, 42(5):387–423, 2001.
- [7] E. J. Crampin, E. A. Gaffney, and P. K. Maini. Reaction and diffusion on growing domains: Scenarios for robust pattern formation. *Bull. Math. Biol.*, 61(6):1093–1120, Nov 1999.

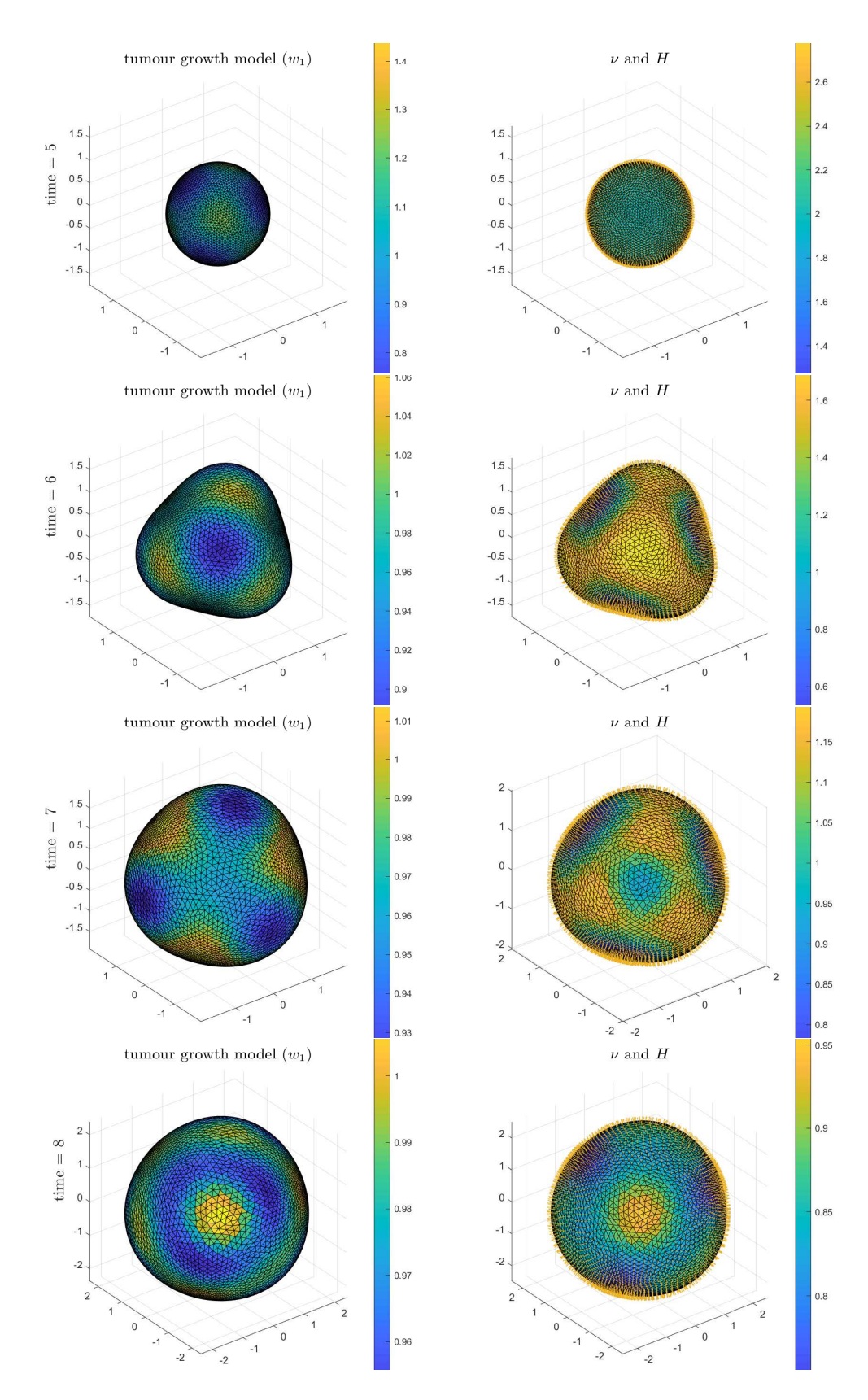


Figure 5: Evolution of the solution (w_1) , normal vector and mean curvature for tumour growth model with $\gamma = 30$ at time t = 5, 6, 7, 8; dof 3882.

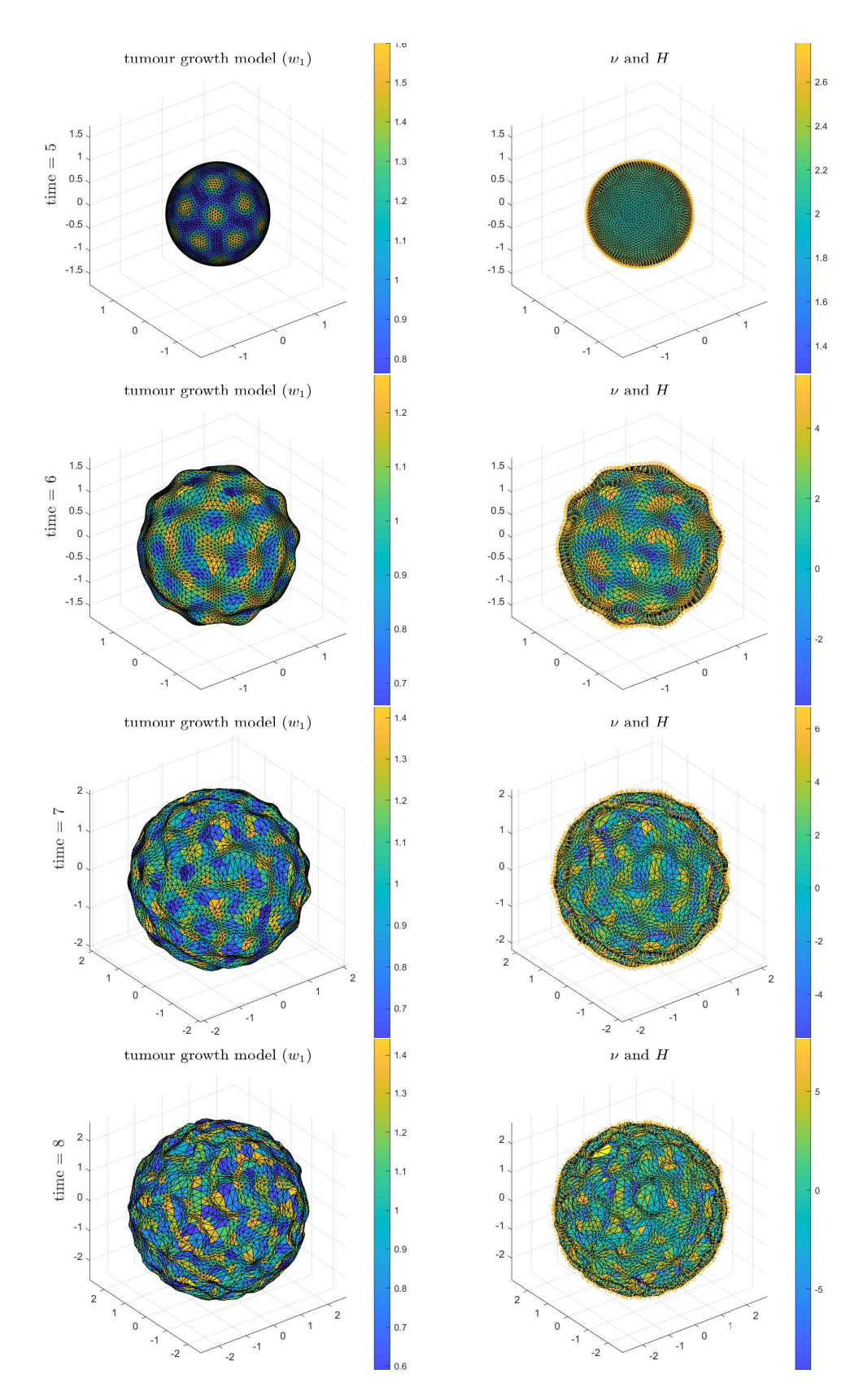


Figure 6: Evolution of the solution (w_1) , normal vector and mean curvature for tumour growth model with $\gamma = 300$ at time t = 5, 6, 7, 8; dof 3882.

- [8] E. J. Crampin, E. A. Gaffney, and P. K. Maini. Mode-doubling and tripling in reaction-diffusion patterns on growing domains: a piecewise linear model. *J. Math. Biol.*, 44(2):107–128, 2002.
- [9] K. Deckelnick, G. Dziuk, and C. M. Elliott. Computation of geometric partial differential equations and mean curvature flow. *Acta Numerica*, 14:139–232, 2005.
- [10] K. Deckelnick, C. Elliott, and V. Styles. Numerical diffusion-induced grain boundary motion. *Interfaces Free Bound.*, 3(4):393–414, 2001.
- [11] A. Demlow. Higher–order finite element methods and pointwise error estimates for elliptic problems on surfaces. *SIAM J. Numer. Anal.*, 47(2):805–807, 2009.
- [12] G. Dziuk. Finite elements for the Beltrami operator on arbitrary surfaces. *Partial differential equations and calculus of variations, Lecture Notes in Math.*, 1357, Springer, Berlin, pages 142–155, 1988.
- [13] G. Dziuk. An algorithm for evolutionary surfaces. *Numer. Math.*, 58(1):603–611, 1990.
- [14] G. Dziuk and C. Elliott. Finite elements on evolving surfaces. *IMA J. Numer. Anal.*, 27(2):262–292, 2007.
- [15] G. Dziuk and C. Elliott. Finite element methods for surface PDEs. *Acta Numerica*, 22:289–396, 2013.
- [16] K. Ecker. Regularity theory for mean curvature flow. Springer, 2012.
- [17] C. Eilks and C. Elliott. Numerical simulation of dealloying by surface dissolution via the evolving surface finite element method. *J. Comput. Phys.*, 227(23):9727–9741, 2008.
- [18] C. M. Elliott and H. Fritz. On approximations of the curve shortening flow and of the mean curvature flow based on the DeTurck trick. *IMA J. Numer. Anal.*, 37(2):543–603, 2017.
- [19] J. Erlebacher, M. Aziz, A. Karma, N. Dimitrov, and K. Sieradzki. Evolution of nanoporosity in dealloying. *Nature*, 410(6827):450, 2001.
- [20] P. Fife, J. Cahn, and C. Elliott. A free-boundary model for diffusion-induced grain boundary motion. *Interfaces Free Bound.*, 3(3):291–336, 2001.
- [21] E. Hairer and G. Wanner. Solving Ordinary Differential Equations II. Stiff and Differential—Algebraic Problems. Springer, Berlin, Second edition, 1996.
- [22] G. Huisken. Flow by mean curvature of convex surfaces into spheres. *J. Differential Geometry*, 20(1):237–266, 1984.
- [23] B. Kovács, B. Li, and C. Lubich. A convergent evolving finite element algorithm for mean curvature flow of closed surfaces. *Numer. Math.*, 143:797–853, 2019.

- [24] B. Kovács, B. Li, C. Lubich, and C. Power Guerra. Convergence of finite elements on an evolving surface driven by diffusion on the surface. *Numer. Math.*, 137(3):643–689, 2017.
- [25] B. Kovács and C. Lubich. Linearly implicit full discretization of surface evolution. *Numer. Math.*, 140(1):121–152, 2018.
- [26] C. Lubich, D. Mansour, and C. Venkataraman. Backward difference time discretization of parabolic differential equations on evolving surfaces. *IMA J. Numer. Anal.*, 33(4):1365–1385, 2013.
- [27] L. Mugnai and M. Röger. Convergence of perturbed Allen-Cahn equations to forced mean curvature flow. *Indiana Univ. Math. J.*, 60(1):41–75, 2011.
- [28] P. Pozzi and B. Stinner. Curve shortening flow coupled to lateral diffusion. *Numer. Math.*, *doi:10.1007/s00211-016-0828-8*, 2017.
- [29] V. Styles. An evolving surface finite element method for the numerical solution of diffusion induced grain boundary motion. In *Numerical Mathematics And Advanced Applications 2011*, pages 469–477. Springer, Heidelberg, 2013.
- [30] S. W. Walker. The shape of things: a practical guide to differential geometry and the shape derivative. SIAM, Philadelphia, 2015.